Effect of Sustained Flexural Loading on Self-Healing of Engineered Cementitious Composites

Erdoğan Özbay[1], Mustafa Şahmaran[2], Hasan E. Yücel[2], Tahir K. Erdem[3], Mohamed Lachemi[4], Victor C. Li[5]

Abstract

This paper aims to clarify the effects of sustained flexural loading on the self-healing behavior of Engineered Cementitious Composites (ECC). Prismatic specimens of ECC mixtures with two different levels of Class-F fly ash content were cast. Flexural loading was applied to the specimens at 28 days age to generate severe amount of microcracks. The specimens were then stored under continuous water or air exposures with or without sustained mechanical loading, for up to 90 days. For specimens under sustained mechanical loading, the applied sustained load level was 60% of the ultimate flexural strength. The extent of damage was determined as a percentage of loss in mechanical properties. The influences of different exposure regimes and sustained mechanical loading on mechanical properties of ECC mixtures were investigated. Microstructural changes within the microcracks were also analyzed.

1. Introduction

Self-healing of concrete can be defined as the ability of cracks in concrete to diminish autogeneously in width over time. In a broad sense, the self-healing approaches for concrete could be classified into five categories: chemical encapsulation, bacterial encapsulation, mineral admixtures, chemical in glass tubing and intrinsic self-healing with self-controlled tight crack width (Li and Herbert 2012). Among the approaches for self-healing, the intrinsic natural tendencies of continued reactions under natural environment (rain and air) have been accepted as one of the simplest approaches for the self-healing of cracks in concrete. In concrete infrastructures where water and CO_2 are available, concrete can produce the necessary chemical products to heal its own damage. Self-healing is mainly attributed to the formation of calcium carbonate, which is a result of the reaction between calcium ions in concrete and atmospheric CO_2 dissolved in water (Cowie and Glassert 1992; Edvardsen 1999). This type of self-healing mainly improves transport properties, and is therefore most pertinent to infrastructure such as underground structures, water tanks, water channel and dams where impermeability is important. Continuous hydration of unhydrated cementitious materials is another intrinsic self-healing mechanism (Heide and Schlangen 2007). Due to the limited volume of self-healing products, the crack width of the concrete material has been found to be critical for intrinsic self-healing to take place (Li and Yang 2007; Qian *et al.* 2009). The crack width required to promote self-healing falls roughly below 100 μm, and preferably lower than 50 μm especially for self-healing based on ongoing hydration of unhydrated cementitious materials (Heide and Schlangen 2007; Li and Yang 2007). Narrow crack width is therefore one of the most important criteria for attaining effective intrinsic self-healing in cementitious materials.

During the last decade, concrete technology has been undergoing rapid development. The effort to modify the brittle behavior of plain cement materials such as cement pastes, mortars and concretes has resulted in modern concepts of high performance fiber reinforced cementitious composites (HPFRCC), which are characterized by tensile strain-hardening after first cracking and multiple microcracks with tight crack width. Engineered Cementitious Composites (ECC) is a special type of HPFRCC, micromechanically designed to achieve high damage tolerance under severe loading and high durability under normal service conditions (Li 2003). It is a relatively new material, with a number of benefits, including high ductility under uniaxial tensile loading, and improved durability due to intrinsically tight crack widths. These tight crack widths of ECC also promote the robust self-healing behavior of composites that is not easily attainable in brittle conventional concrete with uncontrolled crack widths (Li and Yang 2007).

In recent years, the intrinsic self-healing ability of both conventional concrete and ECC has been researched under various conditions that affect the amount and rate of self-healing including the various environ-

[1]Department of Civil Engineering, Mustafa Kemal University, Antakya, Turkey.
[2]Department of Civil Engineering, Gaziantep University Gaziantep, Turkey.
[3]Department of Civil Engineering, İzmir Institute of Technology, İzmir, Turkey.
[4]Department of Civil Engineering, Ryerson University, Toronto, ON, Canada.
[5]Department of Civil and Environmental Engineering, University of Michigan, MI, USA.
E-mail: vcli@umich.edu

mental exposures such as high temperature, wetting-drying and freeze-thaw cycles (Reinhardt and Joos 2003; Jacobsen and Sellevold 1996; Şahmaran and Li 2010; Yang *et al.* 2009a; Ozbay *et al.* 2012), type of cementitious materials (Şahmaran *et al.* 2013; Ozbay *et al.* 2013), degree of deterioration (Zhong and Yao 2008), the age of the material (Heide and Schlangen 2007; Yamamoto *et al.* 2010; Edvardsen 1999) and the presence of sustained compressive loading during the crack healing (Heide and Schlangen 2007). From these studies, it was found that maximum healing occurred at earlier age of concrete, and specimens tested under water showed the highest mechanical and transport properties recovery, hence it was concluded that the primary healing mechanism was ongoing hydration and precipitation of calcium carbonate. It was also observed that the mechanical properties of the pre-cracked and then moist cured concrete specimens are recovered to a large extent for cracks loaded in sustained compression, which reduces the distance between the crack faces (Heide and Schlangen 2007).

Recent studies by Boshoff and van Zijl (2007) and Jun and Mechtcherine (2010) indicate that crack width may open wider under sustained loading due to creep mechanisms. Therefore, in addition to the impact of environmental conditions, type of cementitious materials, degree of deterioration, pre-loading age, and the presence of sustained compressive loading on self-healing behavior, the influence of sustained flexural loading should also be of interest due to the tendency of wider crack width under sustained mechanical loading. To account for crack closure on unloading, all crack width measurements were generally made in the unloaded state, and the self-healing capacity under different environments was also typically assessed in the unloaded state. Since the crack width of ECC specimens under sustained flexural load (close to or larger than 100 µm) is found to be almost double that of the unloaded specimen (Yang *et al.* 2007; Zhou *et al.* 2010), it is important to examine the self-healing behavior of pre-cracked ECC specimens under sustained flexural loading, which is of great importance for critical assessment of the performance of ECC under comprehensive conditions.

This paper aims to clarify the effect of sustained flexural loading on the self-healing behavior of ECC. For this purpose, two ECC mixtures with two different levels of fly ash content (55 and 70% FA) were produced. ECC prism specimens were preloaded under four-point flexural load to a pre-specified deformation level. After this initial damage was introduced, the ECC specimens placed under sustained flexural loading were exposed to two different exposure regimes (continuous air and continuous water) for up to 90 days to determine residual mechanical properties (flexural stiffness, flexural strength and deflection capacity) after healing (if any). The sustained mechanical load level remained constant due to a special test set-up at 60% of the static ultimate

load-carrying capacity of ECC specimens. To develop an understanding of how the sustained mechanical loading affected self-healing performance, testing of residual mechanical properties of both uncracked and cracked ECC reference specimens without sustained mechanical loading was performed under similar exposure regimes. In addition to a study of the recovery of mechanical properties, microstructural changes within the cracks were also analyzed.

2. Experimental program

2.1 Materials, mixture proportions, and basic mechanical properties

Two ECC mixtures were prepared in a standard mortar mixer with a water to cementitious material (W/CM) ratio of 0.27 and fly ash to cement ratios (FA/C) of 1.2 and 2.2, by mass (ECC-1 and ECC-2). The mixture proportion of an ECC with FA/C ratio of 1.2 is referred to as a "standard" mixture in the literature (Yang *et al.* 2007), and has the largest experimental dataset published to date. Composition details are provided in **Table 1**. The components of the ECC mixtures were similar to typical fiber-reinforced cement composites, and consisted of CEM I 42.5 type Portland cement, sand, Class-F FA, water, fibers, and a high-range water-reducing admixture (HRWR). The chemical composition and physical properties of cement and FA are presented in **Table 2**.

Table 1 Mixture properties of ECC.

Ingredients	ECC-1	ECC-2
Cement (C), (kg/m^3)	558	375
Fly ash (FA), (kg/m^3)	669	823
Water, (kg/m^3)	326	318
PVA fiber, (kg/m^3)	26	26
Sand, (kg/m^3)	446	435
HRWR, (kg/m^3)	5.1	3.0
W/(C+FA)	0.27	0.27
FA/C	1.2	2.2

Table 2 Chemical and physical properties of cement and fly ash.

Chemical composition	Cement	Fly Ash
CaO (%)	61.43	1.64
SiO$_2$ (%)	20.77	56.22
Al$_2$O$_3$ (%)	5.55	25.34
Fe$_2$O$_3$ (%)	3.35	7.65
MgO (%)	2.49	1.80
SO$_3$ (%)	2.49	0.32
K$_2$O (%)	0.77	1.88
Na$_2$O (%)	0.19	1.13
Loss on ignition (%)	2.20	2.10
SiO$_2$+Al$_2$O$_3$+Fe$_2$O$_3$	29.37	89.21
Physical properties		
Specific gravity	3.06	2.31
Blaine fineness (m^2/kg)	325	290

To minimize the matrix fracture toughness advantageous for composite tensile ductility, no large aggregates were used, and silica sand with a maximum grain size of 400 μm was incorporated. The polyvinyl alcohol (PVA) fibers had an average diameter of 39 μm, an average length of 8 mm, a tensile strength of 1620 MPa, an elastic modulus of 42.8 GPa, and a maximum elongation of 6.0%. In accordance with micro-mechanics based design theory of ECC, a very strong interface bond leads to fiber rupture at small crack opening, resulting in small complementary energy (Li 2003). High complementary energy is essential to achieve strain-hardening, and higher complementary energy leads to more saturated multiple cracking. Due to the strongly hydrophilic nature of PVA, the fiber surfaces were coated with an oiling agent (1.2% by weight) to reduce the interfacial bond strength between the fiber and matrix, and minimize fiber rupture (Li 2003). HRWR was added to the mixture until the desired fresh ECC characteristics, described in another study (Yang *et al*., 2009-b), were visually observed.

For the determination of the flexural and compressive strengths, several 360×50×75 mm prism and 50-mm cube specimens were prepared. All specimens were demolded at the age of 24 hours, and moisture cured in plastic bags at 95±5% RH, 23±2 °C for seven days. The specimens were then air cured in a laboratory setting at 50±5% RH, 23 ±2 °C until the age of 28 days. The compressive strength test results for ECC mixtures at 28 days are listed in **Table 3**. A minimum of five compression cubes was used to obtain the average compressive strengths, following ASTM C39 procedures. As seen from **Table 3** and as expected, the compressive strength of ECC decreased with increasing FA content; however, even at almost 70% replacement of Portland cement with FA (FA/C = 2.2), the compressive strength of ECC-2 at 28 days was over 45 MPa.

The four-point bending test was performed on a closed-loop controlled material testing system at a loading rate of 0.005 mm/s. 360×50×75 mm prism specimens from each mixture were prepared to determine the ultimate flexural strength and mid-span beam deflection capacity. The span length of flexural loading was 304 mm, with a 101 mm center span length. Two LVDTs were fixed to the flexural test set-up at the beam mid-span on both sides of beam mid-span to measure flexural deformation. Load and mid-span beam deflection capacity were recorded on a computerized data recording system. At the end of the 28 days, six prism specimens from each mixture were tested under the four-point bending test up to failure, and the average flexural stiffness, ultimate flexural strength and mid-span beam deflection capacity of each mixture was determined. The flexural stiffness is defined as the secant of the initial rising branch of the flexural stress-deflection curve, in which the first point is chosen at 1 MPa and the second point at 5 MPa for both mixtures. Between these two stress points, the slope is almost linear for all cases. The deflection capacity was defined as the deflection at which point the bending stress reaches maximum (modulus of rupture). The typical flexural stress-mid-span deflection curves of the ECC mixtures at the age of 28 days are shown in **Fig. 1**.

The test results in terms of average flexural strength, mid-span beam deflection capacity and flexural stiffness of uncracked ECC specimens at 28 days are displayed in **Table 3**. It is evident that increasing FA/C ratio improves the deformation capacity (ductility) of ECC. It is also apparent from **Table 3** that unlike compressive strength, FA replacement rate does not significantly in-
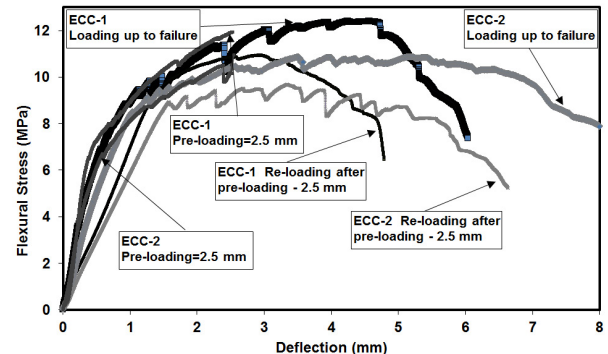

Fig. 1 A typical flexural stress-deflection curves for preloading and re-loading ECC specimens at 28 days of age.

Table 3 Mechanical properties of unhealed specimens at 28 days of age.

Mechanical Properties		ECC-1		ECC-2	
		uncracked	2.5 mm pre-loaded	uncracked	2.5 mm pre-loaded
Compressive Strength (MPa)		69.3	-	46.1	-
Flexural strength (MPa)		12.40	10.36	10.07	9.06
Mid-span beam deflection (mm)		4.95	2.55	6.01	3.51
Flexural stiffness (MPa/mm)		13.8	9.5	10.1	7.7
Loaded crack width μm	Max.	-	∼165		∼103
	Min.	-	∼44		∼30
	Ave.	-	∼115	-	∼85
Unloaded crack width μm	Max.		∼110		∼70
	Min.		∼27		∼15
	Ave.	-	∼60	-	∼40
Number of cracks		-	30-39	-	43-50

fluence 28-day flexural strength. This difference can be attributed to the fact that flexural strength is governed by more complex material properties, such as first cracking strength, ultimate tensile strength, matrix toughness and ductility, particularly in the case of strain-hardening cementitious materials (Zhou *et al.* 2010; Wang and Li 2007). Further details concerning the effect of FA on mechanical properties of ECC can be found in Refs. (Wang and Li 2007; Yang *et al.* 2007; Şahmaran and Li 2009).

2.2 Pre-cracking and exposure conditions

To study the self-healing of microcrack damage, some of the prism specimens were pre-loaded up to 2.5 mm mid-span beam deflection value at the age of 28 days to deliberately introduce a number of microcracks. A typical flexural stress–deflection curve obtained when the specimens were mechanically pre-loaded up to 2.5 mm deflection value at 28 days is shown in **Fig. 1**. As seen from **Fig. 1**, the deflection of 2.5 mm was well below the ultimate deflection capacity of both mixtures (close to or higher than 5 mm), with no localized fracture. When the applied mid-span beam deflection level reached 2.5 mm, the load was released and the specimens were removed from the test machine to prepare for different exposure and reloading schemes. **Figure 1** shows typical flexural stress-deflection curves of ECC specimens pre-cracked to a 2.5 mm deflection level, unloaded, then immediately reloaded, leaving them no time to undergo any crack healing. **Table 3** presents the 28-day mechanical properties of ECC specimens that were previously pre-loaded to a beam deflection level of 2.5 mm.

In order to study the effect of crack healing under sustained mechanical loading, microcracks were initially produced in ECC specimen in a controlled manner, as explained above. The specimen was then unloaded and removed from the machine. After unloading, the crack opening decreased, but did not completely close (**Fig. 2**). At this moment, the specimen was put in a sustained loading device to apply a load that would open
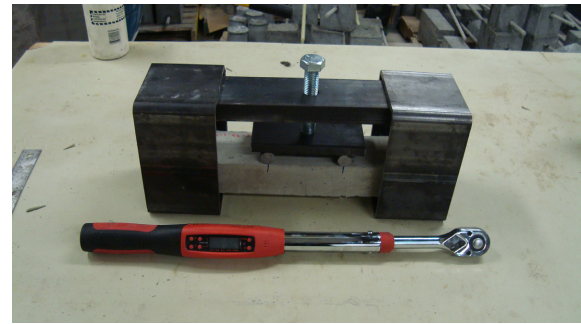

Fig. 3 Four-point sustained flexural loading test set-up.

the crack again. **Figure 3** shows the arrangement for sustained mechanical loading of the prism specimen. The loading level remained constant throughout the tests at 60% of the flexural ultimate load. Each beam was supported on a pair of steel rollers and the load was applied through two similar rollers mounted at the one-third points of the supporting span. The specimens were loaded using threaded rods; a torque wrench was used to tighten the rods. To evaluate the load placed on the specimens, a load cell was initially inserted in place of the specimen, and torque was applied by a torque wrench, which was then calibrated against the load cell. It is important to note that almost no stress relaxation was observed in any of the specimens under sustained mechanical loading over a period of 90 days.

As mentioned earlier, cracks partially close on unloading. To account for this occurrence, all crack widths were measured for all specimens in both loaded and unloaded stages. For each specimen, two lines parallel to the longitudinal axis of the beam were drawn on the cracked surface. The number of cracks and crack width was measured over these lines using a video microscope (maximum enlargement of 125X) for unloaded specimens and portable microscope for both unloaded and loaded specimens. The crack characteristics of ECC specimens were tabulated in **Table 3** in terms of crack number, and minimum, maximum and average crack width measurements on pre-cracked prism specimens with and without mechanical loading. As a result of
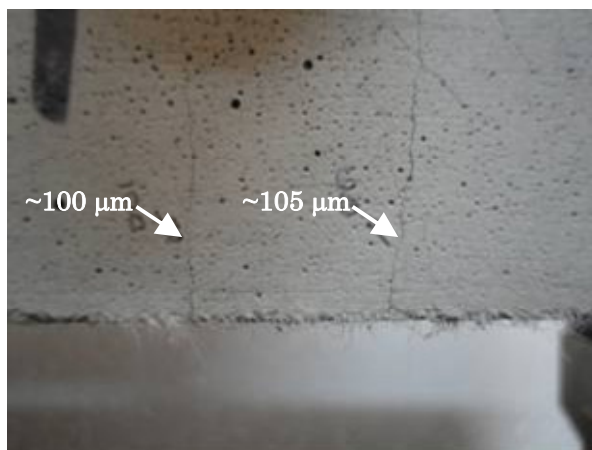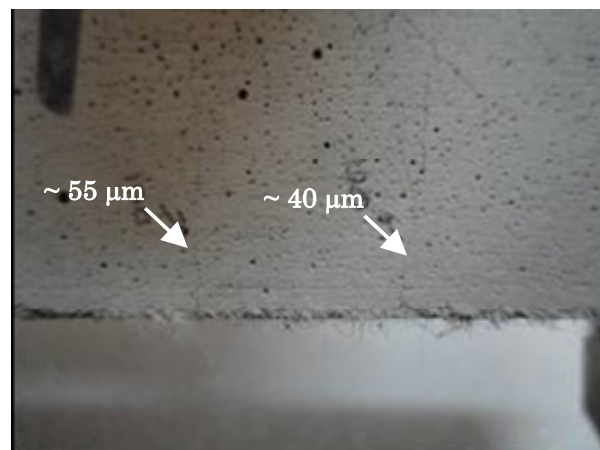
Loaded | Unloaded

Fig. 2 Crack characteristics of ECC specimens with or without mechanical loading.

flexural tensile pre-loading to ECC prism specimens, in addition to cracks with the widths between 30 and 115 μm, many cracks with width less than 20 μm (especially in ECC-2 mixture) were also observed. It was also found that crack width was reduced and crack numbers were increased as fly ash content increased at all ages. Average crack width was about 60 μm for unloaded ECC-1 and 40 μm for ECC-2. The improvement in the crack width with the increase in the FA content can be attributed to the fact that the increase in the FA content tends to reduce the fiber/matrix interface chemical bond and matrix toughness, while increasing the interface frictional bond, in favor of obtaining more robust multiple micro-cracking behavior (Wang and Li 2007; Yang *et al*. 2007; Şahmaran and Li 2009). It was also observed that the average crack width of a loaded specimen is approximately two times that of the unloaded specimen (see **Table 3**), a finding that is consistent with previous studies (Yang *et al*. 2007; Zhou *et al*. 2010).

After this step, the pre-loaded ECC specimens were stored in specific exposure conditions (aging) along with uncracked (sound) specimens with and without sustained mechanical loading. The overall program for four-point bending testing after 28 days of age is shown in **Fig. 4**, and includes data on two different exposure regimes, two different loading schemes, and number of specimens tested under each condition. Two different exposure periods are shown: 30 and 90 days. Specimens aged in water were completely immersed in stationary tap water at 23±2 °C to simulate underwater structures, with no water renewal. Specimens aged in air were stored at 23±2 °C and 50±5% RH. The results of the uncracked ECC specimens from this scheme form a reference value to determine how much healing has oc-

curred in terms of deflection capacity, strength and flexural stiffness. After each period of exposure, the last step of the experimental program consisted of reloading the pre-damaged and uncracked specimens under four-point bending to characterize residual mechanical behavior.

The second method used to assess self-healing in this study incorporated a scanning electron microscope (SEM) to observe self-healing products. X-ray energy dispersion (EDX) technique was also used to chemically analyze healing products. The samples with the thickness of 1 cm for SEM observation were obtained from the cracked surface of self-healed ECC specimens by using a thin-bladed low-speed precision circular saw. The specimens with the thickness of 1 cm were then cleaned with pressurized air to remove the dust particles deposited on the surface. For each mixture and exposure period (30 and 90 days), two samples were analyzed under SEM. During SEM examination, an interior spot was examined to assure self-healing in the bulk of the specimen and not just on the surface.

To evaluate the quantity of calcium hydroxide (CH), the corresponding ECC paste samples were also prepared adopting the same proportions. The pastes were cured in plastic bag as in the ECC specimens. The CH content of corresponding ECC pastes samples was determined at 28 days of age by thermal gravimetric analysis (TGA) using Perkin Elmer Diomand TG/DTA device and calculated based on the ignited weight of the sample.

3. Results and discussions

3.1 Recovery of mechanical properties of ECC specimens through self-healing
Flexural stress - deflection curves and flexural stiffness:
Table 4 presents flexural test results from both uncracked specimens and those subjected to preloading at the age of 28 days and later stored up to 90 days in water or air. Each value in **Table 4** is the average of four or six specimens. It is important to note that the coefficient of variations of all the flexural stiffness test results is less than 5%. The coefficient of variance (COV) values for the flexural strength and mid-span beam deformation capacity values ranged from 4.8-7.1% and 6.3-11.4%, respectively. The narrow range of COV values is an indication of the consistent repeatability of the flexural test method.

Figure 5 shows the typical flexural stress – deflection curves obtained for beam specimens subjected to different exposure regimes and different loading schemes. The average curves of reloading for each type of ageing are represented in this figure. Typical flexural stress-deflection curves of the uncracked ECC specimens (air exposure) are also included. As seen from **Fig. 5**, both mixtures behaved similarly under flexural tensile test after 90 days in water or air. As expected, the uncracked
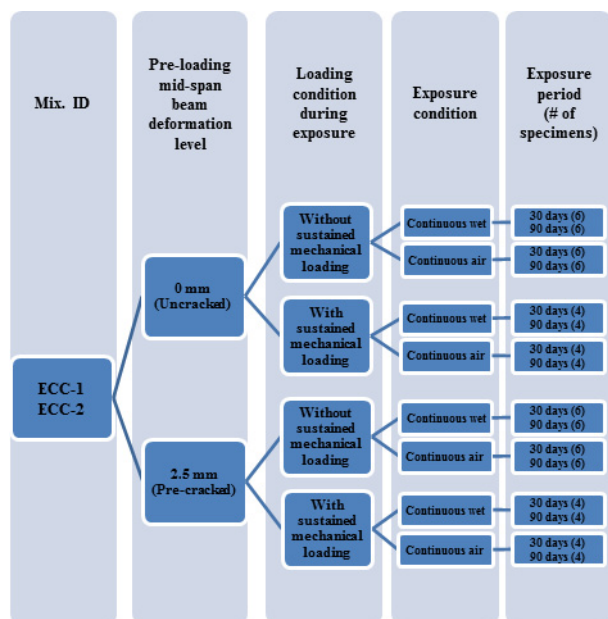

Fig. 4 Four-point bending test program. All specimens underwent 7 days moist curing followed by air curing prior to pre-loading at 28 days.

Table 4 Flexural properties of ECC mixtures.

Specimen type		Deflection (mm)				Flexural Strength (MPa)				Flexural Stiffness (MPa/mm)				Number of Cracks**			
		30 d.		90 d.		30 d.		90 d.		30 d.		90 d.		30 d.		90 d.	
		AE*	WE*	AE	WE	AE	WE	AE	WE	AE	WE	AE	WE	AE	WE	AE	WE
ECC-1		without sustained mechanical loading															
	Uncracked	4.55	4.20	4.48	4.12	12.7	12.3	12.8	12.4	14.3	16.1	15.0	17.6	-	-	-	-
	2.5 mm	2.70	3.80	2.86	3.71	10.6	11.9	10.9	12.1	10.0	12.5	10.5	15.3	29-38	23-29	28-37	5-11
		with sustained mechanical loading															
	Uncracked	4.46	4.11	4.40	4.03	12.5	12.1	12.5	12.4	14.0	15.8	14.9	17.1	-	-	-	-
	2.5 mm	2.60	3.05	2.63	3.24	10.2	11.1	10.5	11.8	9.4	11.6	9.6	13.3	30-39	26-31	30-39	7-14
ECC-2		without sustained mechanical loading															
	Uncracked	5.80	5.33	5.53	5.11	11.4	11.1	11.6	11.4	11.1	13.2	11.7	15.2	-	-	-	-
	2.5 mm	3.67	5.04	3.73	4.73	9.4	11.0	9.9	11.3	8.7	12.0	9.2	14.5	40-47	11-19	38-46	2-7
		with sustained mechanical loading															
	Uncracked	5.66	5.25	5.47	4.96	11.3	11.0	11.5	11.3	10.7	12.8	11.3	14.9	-	-	-	-
	2.5 mm	3.59	4.37	3.64	4.64	9.2	10.5	9.3	11.1	8.2	10.5	8.7	12.6	43-50	15-24	43-50	4-11

AE: Air Exposure, WE: Water Exposure. All specimens underwent 7 days moist curing followed by air curing until 28 days, *before indicated environmental exposures.*

** Number of cracks shows the crack number observed under the microscope just before the flexural strength testing.*
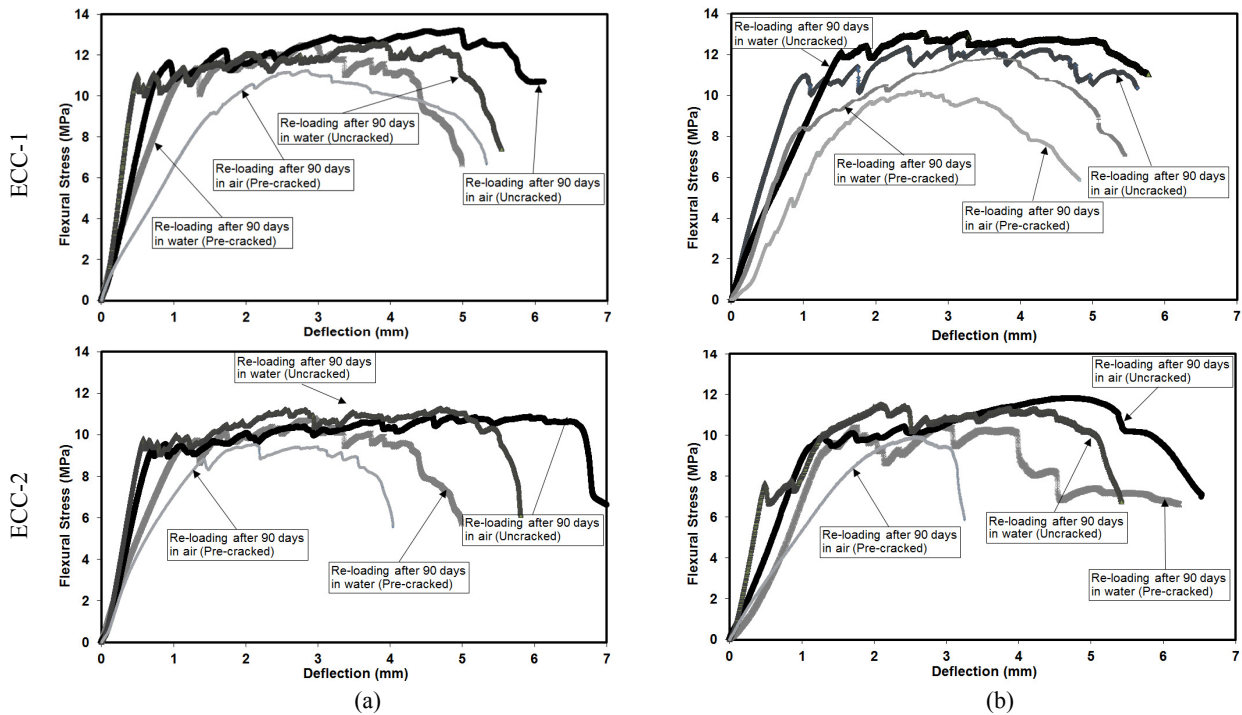

Fig. 5 Effects of different exposure and loading conditions on flexural stress-displacement behavior of ECC mixtures: (a) without and (b) with sustained mechanical loading.

samples exposed to air or water (reference samples) showed a typical deflection hardening behavior of HPFRCC (increase in deformation after first cracking with increasing load carrying capacity) for both mixtures at all ages. The deflection curve for uncracked specimens under different exposure conditions and loading schemes is characterized by an initial linear curve up to about 90% of ultimate flexural strength, followed by a bend and subsequent plateau curve with a slight positive slope. The large nonlinear portion of the deflection curve corresponds to the continuous microcracking process of the specimens.

In terms of the effect of further water exposure up to 90 days beyond preloading at 28 days, significant recovery of the flexural stress-displacement curve of the pre-cracked ECC specimens has been accomplished (see the curves of "re-loading after 90 days in water (pre-cracked)" in **Fig. 5**). Similarly, the load-deflection curves of water exposed pre-cracked specimens reveal the characteristics of deflection hardening behavior, resulting in a more or less linear curve followed by a plateau curve. The visual observations made during
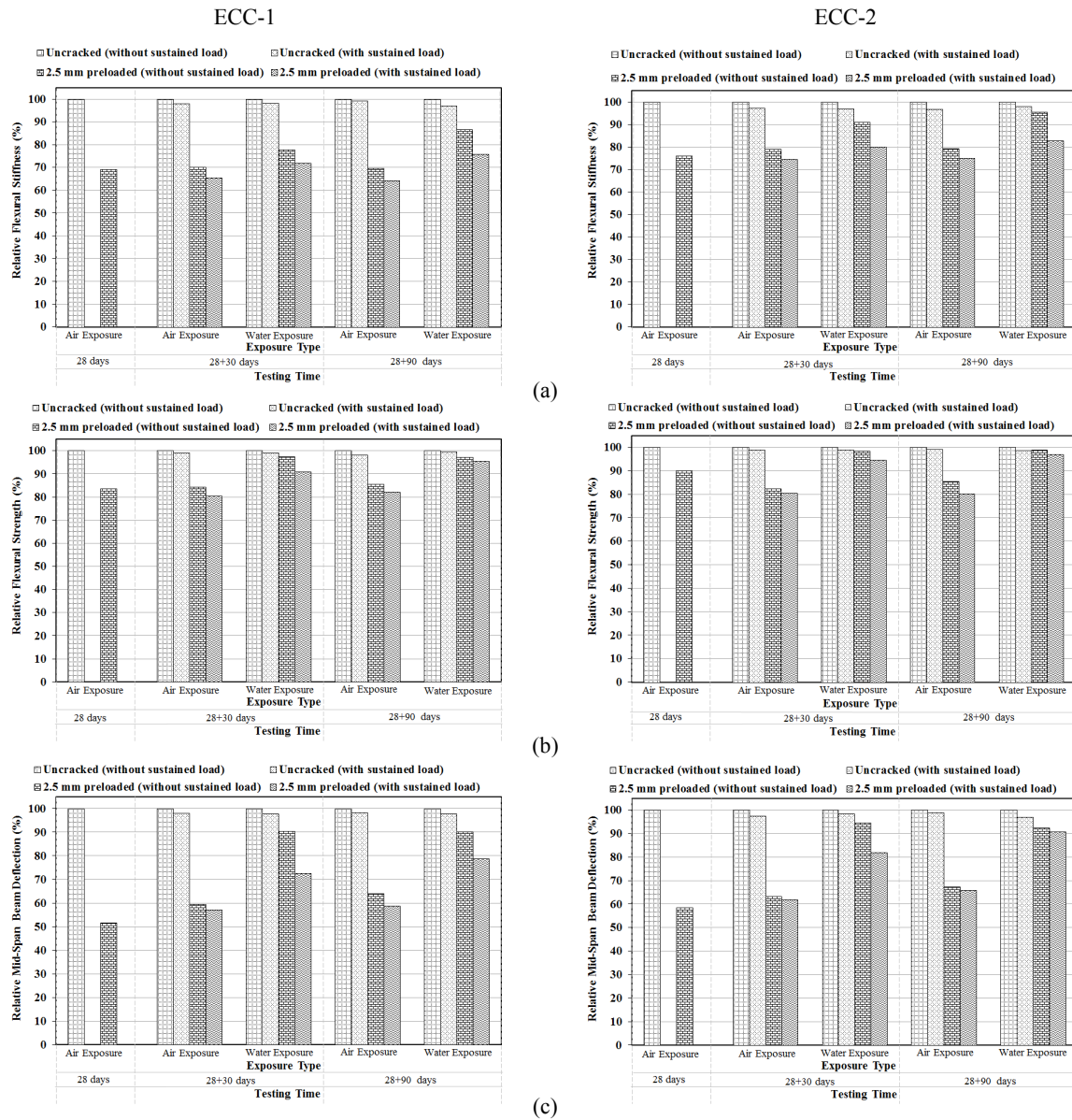
Fig. 6 Influence of different exposure regimes and sustained mechanical loading on mechanical properties of ECC mixtures: (a) Flexural stiffness, (b) Flexural strength, and (c) Flexural deformation capacity.

flexural testing revealed that the linear curve for healed specimens is largely due to reopening of microcracks from previous loading. For this reason, the initial linear portion of the flexural stress-deflection curves of the pre-cracked specimens extends only up to about 70% of the ultimate load. The plateau is the result of additional cracking from new defect sites and relatively strong self-healed cracks. For the pre-cracked specimens, sustained mechanical loading during exposure appears to significantly decrease the re-healing process.

In contrast to water exposed pre-cracked specimens, little sign of deflection hardening in the pre-cracked specimens stored in air (see the curves of "re-loading after 90 days in air (pre-cracked)" in **Fig. 5**) was observed. As soon as the linear stage ends, the deflection curve bends and localized fracture failure occurs shortly

thereafter. This suggests that few new cracks developed; most cracks can be attributed to the reopening of old microcracks from pre-loading. As seen from **Table 4**, all flexural properties of pre-cracked specimens stored in air with sustained mechanical loading are lower than those of pre-cracked specimens stored in air without sustained mechanical loading. Therefore, the application of sustained mechanical loading appears to exacerbate deterioration or limit the recovery of mechanical properties as a result of self-healing.

Figure 6a shows the stiffness of ECC specimens as a percentage of the stiffness of the uncracked specimens exposed to the same regime (water or air) without sustained mechanical loading at a particular age. Both **Fig. 6a** and **Table 4** show slight or almost no stiffness gain upon reloading for specimens stored in air. Therefore,

these specimens clearly exhibited no self-healing. The reloading stiffness without self-healing indicates the stiffness of the relatively soft bridging fibers. On the other hand, a significant recovery of mechanical stiffness was achieved for the pre-cracked samples exposed to water without sustained mechanical loading; stiffness of the specimens approaches that of the uncracked specimens. The recovery in material stiffness is more evident for ECC-2 specimens. For example, the relative stiffness of pre-cracked ECC-2 (FA/C=2.2) specimens improves to over 95% when exposed to 90-day water exposure. This value is on the order of 86% for ECC-1 (FA/C=1.2) specimens. These results indicate clearly that new rehealing products, with stiffness close to that of products with normal hydration, have precipitated in cracks and mechanically bind the crack faces. This suggests that between induced pre-cracking and reload testing, and after continuous immersion in water, healing of the microcracks occurred. Moreover, increase in FA content further improved the self-healing capacity of ECC, a fact that can be attributed primarily to the tighter crack width in the ECC-2.

Under sustained mechanical loading, the level of stiffness of pre-cracked specimens after air and water exposure decreases when compared with the specimens exposed to the same environment but without sustained mechanical loading for both mixtures (**Fig. 6a**). This result is likely due to the increased average crack width caused by sustained loading, as discussed in the previous section. The larger average crack width contributes to reduced healing and stiffness recovery.

Flexural strength:
Figure 6b compares the relative flexural strength of mixtures ECC-1 and ECC-2 under air and water exposure conditions and with and without sustained mechanical loading schemes. In terms of relative flexural strength, **Fig. 6b** shows the flexural strength of ECC specimens as a percentage of the strength of the uncracked specimens exposed to the same condition without sustained mechanical loading at a particular age. Since the ultimate flexural strength for both mixtures was not reached during pre-cracking at the age of 28 days, the final fracture plane which dominates flexural strength did not open during the pre-cracking process. Therefore, unlike flexural stiffness, the amount of measurable damage and healing were least reflected by flexural strength, as revealed in **Fig. 6b**.

For the control ECC mixture (with 55% FA, ECC-1) that did not go through any healing, preloading up to a 2.5 mm deflection level caused a strength reduction of about 17% (**Fig. 6b**). As expected, almost no increase in strength was observed under air exposure (see **Table 4**). However, with subsequent exposure in water without sustained mechanical loading, the strength almost completely recovered, even after only 30 days. Under sustained mechanical loading, strength reduction came down from 20% to about 10% in the first 30 days, and

to 5% in the next 90 days under water exposure. For ECC-2 mixture, the flexural strength reduction due to preloading was 10% at 28 days. With subsequent water exposure but without sustained loading, it was reduced to 2% in the first 30 days, and then to 1% in the next 60 days. For the same mixture under sustained mechanical loading, strength reduction came down from 10% to about 5% in the first 30 days, and to 3% in the next 60 days.

Based on the above-mentioned results, it was observed that the reduction in flexural strength of the control ECC mixture (ECC-1) after preloading damage was more than that of ECC mixtures with higher FA content (ECC-2). In addition to the tighter crack width in the ECC-2 mixture, this may also be attributed to the observation that increased FA content caused an increase in the ductility of the composite. ECC-1 specimens with ultimate deflection capacity of 4.95 mm at the age of 28 days had a relatively higher damage levels (closer to failure) as a result of the 2.5 mm pre-loading deflection than ECC-2 specimens with ultimate deflection capacity of 6.01 mm at the age of 28 days. The amount of fly ash apparently influenced strength loss due to pre-cracking and the extent of self-healing of the pre-cracked ECC specimens, even after 30 days of wet exposure.

Deformation capacity:
Deformation capacity/ductility is of major concern for HPFRCC such as ECC, since their structural application specifically takes advantage of their high ductility (Lepech and Li 2009). **Table 4** summarizes the average flexural deformation capacity of ECC specimens stored in continuous air and water exposure regimes with and without sustained mechanical loading. The flexural deformation capacity reported for these specimens does not include the residual flexural deformation from the pre-cracking load. By neglecting this residual deflection, the significant variability in material relaxation during unloading is avoided, and a conservative estimation for ultimate deflection capacity of the material is presented.

As shown in **Table 4**, the deformation capacity of uncracked specimens without sustained mechanical loading decreased slightly with time due to the continuous evolution of matrix and fiber/matrix interface properties. However, a stable deformation capacity is eventually expected due to the maturity of matrix and fiber/matrix interface properties. This has been confirmed in a long-term durability study of ECC by Şahmaran and Li (2009); their results indicate a stable ductility after about three months. **Table 4** also shows that for uncracked specimens, sustained mechanical loading during different exposure regimes does not appear to negatively affect deformation capacity. Moreover, the water exposed uncracked samples showed lower deflection capacity compared with the air exposed samples.

Figure 6c presents the relative deformation capacity of the specimens after healing with and without sustained loading during exposure period. The relative de-

flection is shown as the percentage of the deflection of the uncracked specimens exposed to the same condition without sustained mechanical loading at a particular age. As seen in this figure, under water exposure, pre-cracked samples of both mixtures without sustained loading almost fully recovered their deflection capacity, even after 30 days of exposure. This is significant, especially when considering the fact that these samples had been pre-cracked to 2.5 mm deflection.

Figure 6c also shows that with sustained mechanical loading on the pre-cracked specimens, there was a significant decrease in deflection recovery under water exposure. Moreover, this effect was more pronounced for ECC-1 specimens, which may be attributed to the fact that ECC-2 specimens (FA/PC=2.2) have tighter crack width than ECC-1 (FA/PC=1.2). As shown in **Table 4**, the average crack width of ECC-1 specimens under sustained loading remained more than 100 μm, which can negatively influence the self-healing process. The better performance of cracked ECC-2 specimens was due not only to tight crack width but also to the presence of a higher amount of unhydrated cementitious material. As FA content is higher in ECC-2 compared to ECC-1, the reservoirs of unreacted cementitious material is also higher in ECC-2, making the self-healing relatively more complete. The authors believe that formation of calcium carbonate and ongoing hydration including pozzolanic reaction are the mechanisms for crack healing that led to deflection recovery in this investigation. It is important to note that the self-healing mechanism based on ongoing hydration only works when the distance between the crack faces is small enough (Şahmaran and Li 2010), as in the ECC-2 specimens with and without sustained mechanical load, and in the ECC-1 specimens without sustained load.

3.2 Crack characteristics and microstructure of self-healed ECC

Crack characteristics of the ECC specimens were investigated for all exposure conditions. At the age of 28 days, as a result of bending loading, the ECC-2 (FA/C=2.2) samples had a larger number of cracks, but a tighter average crack width compared to the ECC-1 samples (**Table 3**). **Figure 7 (a** and **b)** shows the typical crack damage on an ECC specimen after being subjected to 2.5 mm flexural pre-loading. **Figure 7 (c-f)** displays an image of the same location after continuous water exposure. Since no healing was observed in air exposed pre-cracked specimens, only specimens aged under water were shown in **Fig. 7**. After the initial 28-day exposure procedure, exposing the preloaded specimens without sustained mechanical loading under continuous water conditions up to 90 days decreased the number of cracks and average crack widths of both ECC mixtures (**Table 4**). The average crack width and number decreased according to FA content and crack width. For instance, the average crack width of the preloaded specimens under 30 days continuous water exposure decreased from 60

to 40 μm for the ECC-1. Increasing the exposure time up to 28+90 days resulted in a remarkable decrease in crack widths and numbers. The reduction in crack width and number with water exposure was more pronounced for ECC-2 specimens.

While most of the cracks in both mixtures (with width ranging from 10 to 40 μm) healed fully, cracks with a relatively large width of more than 60 μm showed only partial healing, as illustrated in **Fig. 7**. The partially healed crack in **Fig. 7** (**c** and **e**) suggests that the healing products grow from both surfaces of the crack towards the middle. Therefore, the lower self-healing performance of the water exposed pre-cracked specimens under sustained mechanical loading is associated with the wider crack width of ECC specimens. For both mixtures, most of the cracks with width of less than 30 μm were totally closed by newly formed products after the exposure of continuous water (**Fig. 7**).

Figure 8 shows a SEM close-up view of the healing product on the cracked surface of self-healed ECC specimens. An interior spot was chosen for this examination to assure self-healing in the bulk of the specimen and not just on the surface. Similar self-healing products were observed in both ECC mixtures. After 30 days continuous water exposure, crystal formation was observed in cracks. The surface chemical composition analysis based on EDX reveals that the main composition of the healing products inside the microcrack at the age of 30 days is calcium carbonate, which is typically weaker than of the composition of C-S-H gels from the hydration of unhydrated cementitious materials (**Fig. 8a**). Even though calcium carbonate formation is weaker than hydration products of unhydrated cementitious materials, as seen from **Table 4**, it contributes to the recovery of mechanical properties of pre-cracked specimens. The possible reasons for the difference in self-healing in ECC with the formation of calcium carbonate compared to previous studies in conventional concrete can be attributed to the fact that: (a) the small crack width in ECC allows more complete healing than for larger cracks, and therefore better recovery of mechanical strength, and (b) the $CaCO_3$ formation is "reinforced" by the micro-fibers in ECC, as opposed to just the brittle $CaCO_3$ formation in conventional concrete healing. Similar results were also found in the literature (Qian *et al.* 2009).

Intuitively, calcite formation might be suppressed by the high FA content that consumes more of the CH during pozzolanic reaction. The CH content and normalized CH with respect to the proportion of Portland cement present in hardened ECC pastes was determined by TGA at the age of 28 days (at the age of pre-cracking), and the results are given in **Table 5**. TGA results

Table 5 CH content of ECC pastes at 28 days of age.

Mix. ID	CH, %	Normalized CH, %
ECC-1	4.91	10.80
ECC-2	3.55	11.36

(a) ECC-1 cracks before wet exposure

(b) ECC-2 cracks before wet exposure

(c) ECC-1 cracks after 30 days wet exposure

(d) ECC-2 cracks after 30 days wet exposure

(e) ECC-1 cracks after 90 days wet exposure

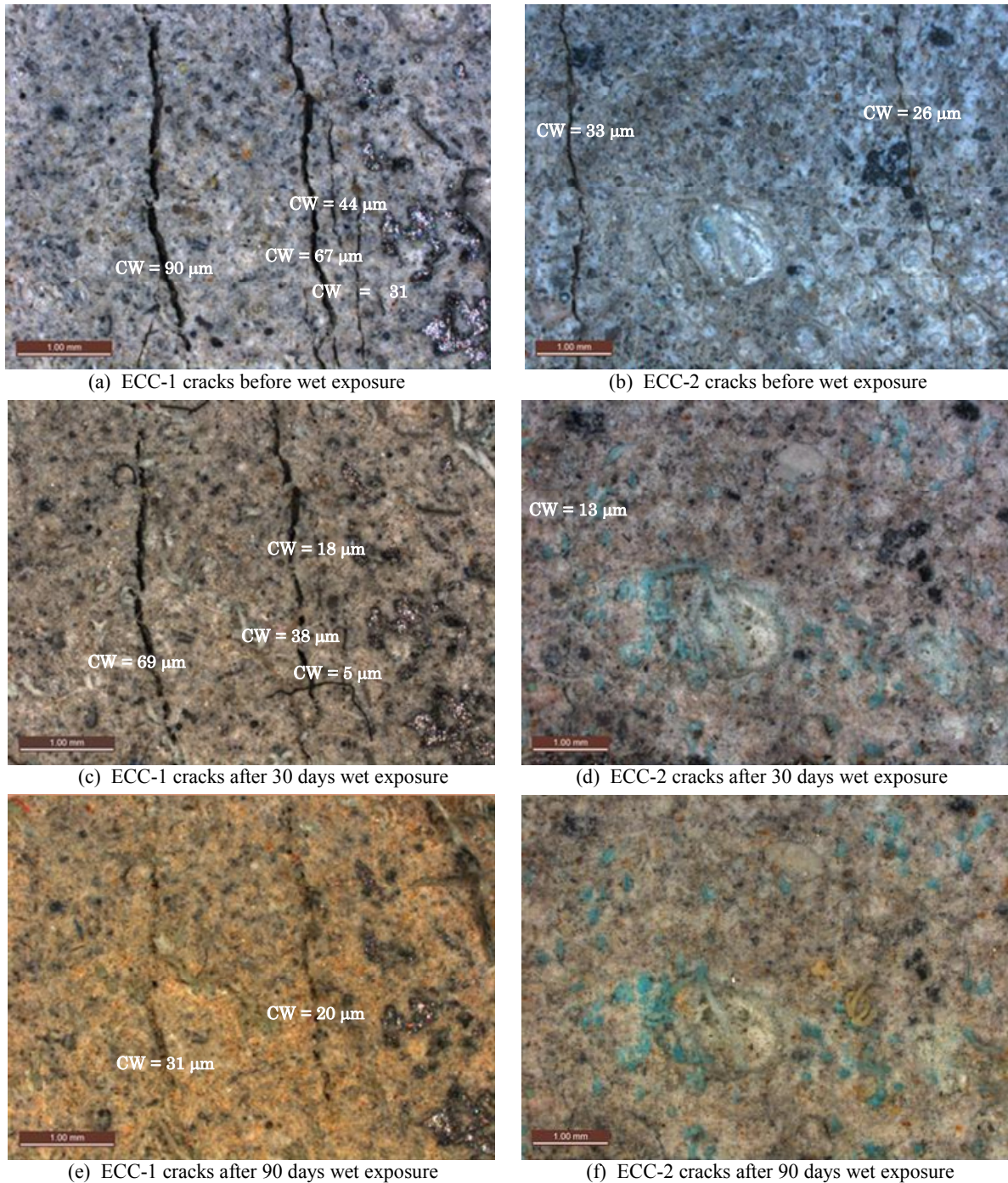
(f) ECC-2 cracks after 90 days wet exposure

Fig. 7 Self-healing products in ECC microcracks before and after continuous water exposure.

showed that significant amount of CH is present in hardened high volume FA-ECC pastes at 28 days. The normalized values of CH content of both ECC mixtures also showed that little amount of CH was consumed at the ages of 28 days by pozzolanic reaction of FA, indicating that pozzolanic action of Class-F FA particles slowly develops at initial stages of hydration. The reason for the determined high amount of CH in high volume FA-ECC mixture at early ages of exposure could be attributed to the fact that ECC specimens were cured in air up to 28-day of age after a 7-day moist curing, and

because of inadequate curing and slower pozzolanic reaction involving FA than cement hydration, most of the FA particles in the matrix remain intact without any chemical reaction with CH. Therefore, with the subsequent water exposure of precracked ECC specimens after 28 days of age, leached calcium ions from the hardened matrix react with the CO_2 dissolved in water to form calcite.

Even though the high amount of unhydrated cementitious material and low W/CM ratio in ECC could have aided in the self-healing process, C-S-H gels were al-
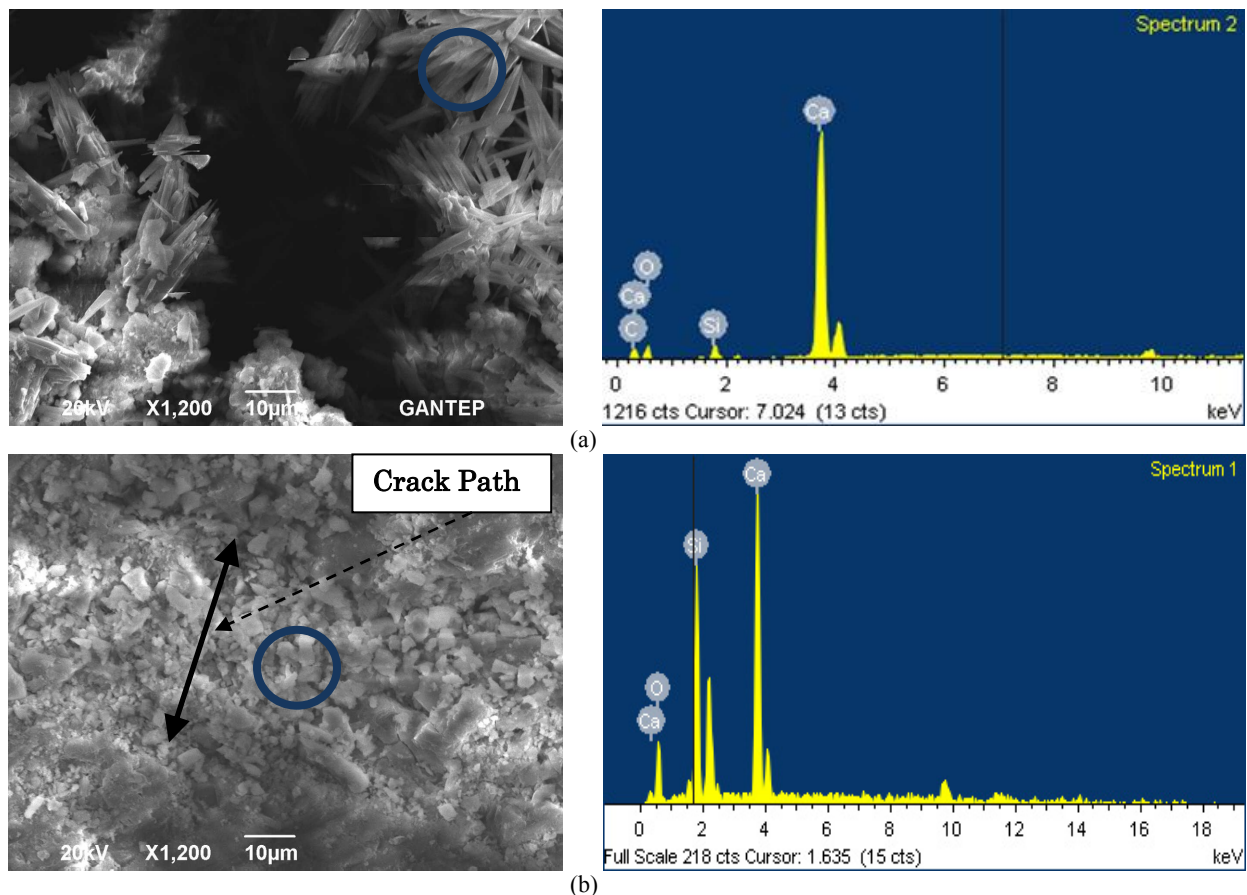
Fig. 8 SEM micrograph with EDX pattern of rehydration products in a self-healed crack of ECC-1 specimen: After (a) 30 days, and (b) 90 days wet exposure.

most not found at early ages of exposure (30 days). After 90 days continuous water exposure, in addition to crystal formation, self-healing product with different morphology was observed at the crack almost fully bridging the cracks with width of less than 50 μm (**Fig. 8b**). EDX results suggest that (**Fig. 8b**) self-healing product with different morphology may be newly formed C-S-H gels formed in the crack path as a result of hydration and pozzolanic reaction. It should be noted that the presence of different hydration and pozzolanic reaction products and calcite formation is difficult to rule out due to the limitations of EDX analysis. Specifically, the interaction volume between the electron beam and the sample may be on the order of 1 $μm^3$ so that information from neighboring phases can bleed into each other. Therefore the EDX analysis should be interpreted with care.

4. Conclusions

The aim of this experimental study is to understand the effect of sustained mechanical loading on the self-healing behavior of pre-cracked ECC specimens. Four-point bending deformation was applied to the 55 and 70% FA-included ECC beam specimens at 28 days of age; these specimens were subsequently exposed to fur-

ther continuous water and air exposure regimes with or without sustained mechanical loading up to 90 days. The effects of sustained mechanical loading and exposure conditions were studied by comparing recovery of the mixtures' mechanical properties (flexural strength, mid-span beam deflection and flexural stiffness).

Specimens submerged in water without sustained mechanical loading showed greatly enhanced flexural stiffness as well as flexural deflection capacity recovery due to the healing products in the microcracks, while this was not the case for air exposed specimens. Self-healing in ECC can be attributed primarily to innately tight crack width, high cementitious material content and relatively low water to binder ratio within the ECC mixture. In a short exposure period (30 days for this study), water exposure promotes the dissolution of calcium hydroxide from the concrete matrix near the crack surface, which is necessary for the formation of calcium carbonate healing products, observed during microstructural analysis. In a longer exposure period (90 days for this study), C-S-H gel from continued hydration of unhydrated cement and pozzolanic reaction of FA particles was also observed filling microcracks in the presence of water.

As for specimens under sustained mechanical loading, the experimental test results show that sustained me-

chanical loading alone had an insignificant effect on the mechanical properties of uncracked specimens stored under different exposure conditions. However, when sustained mechanical loading was applied to the pre-cracked specimens during exposure period, the recovery of mechanical properties as a result of self-healing was reduced. This can be attributed to the fact that the sustained mechanical load caused an increase in the width of the pre-existing cracks in ECC prisms.

Based on the results of the present study, self-healing of microcracks in ECC under water is evident from the mechanical and microstructural properties. However, since the width of crack has been found to be critical for self-healing to take place, the performance obtained from pre-cracked ECC specimens without sustained loading may lead to overestimating the self-healing performance of pre-cracked ECC, resulting in inaccurate predictions. To improve accuracy, future studies of self-healing ECC should properly account for changes in the residual mechanical properties caused by cracking in the presence of sustained mechanical loading.

It is also important to note that many of the findings mentioned above for ECC can also be applicable to other fiber reinforced cement-based composites that achieve tight and distributed cracking at high levels of deformation.

Acknowledgments

References

Boshoff, W. P. and van Zijl, G. P. A. G., (2007). "Tensile creep of SHCC." *In*: H. W. Reinhardt and A. E. Naaman Eds. *Proceedings, Fifth International RILEM Workshop on High Performance Fiber Reinforced Cement Composites* (HPFRCC 5), 87-96.

Cowie, J. and Glassert, F. P., (1992). "The reaction between cement and natural water containing dissolved carbon dioxide." *Advanced Cement Research,* 14(15), 119-34.

Edvardsen, C., (1999). "Water permeability and autogenous healing of cracks in concrete." *ACI Materials Journal*, 96(4), 448-454.

Heide, N. T. and Schlangen, E., (2007). "Self-healing of early age cracks in concrete." *In*: A. J. M. Schmets and S. van der Zwaag Eds., *Proceedings of the first international conference on self-healing materials*, Dordrecht: Springer.

Jacobsen, S. and Sellevold, E. J., (1996). "Self healing of high strength concrete after deterioration by freeze/thaw." *Cement and Concrete Research*, 26, 52-62.

Jun, P. and Mechtcherine, V., (2010). "Behaviour of strain-hardening cement-based composites (SHCC) under monotonic and cyclic tensile loading: Part 1-

Experimental investigations." *Cement and Concrete Composites*, 32(10), 801-809.

Lepech, M. D. and Li, V. C., (2009). "Application of ECC for bridge deck link slabs." *Materials and Structures*, 42(9), 1185-1195.

Li, V. C., (2003). "On engineered cementitious composites (ECC) - A review of the material and its applications." *Journal of Advanced Concrete Technology*, 1(3), 215-230.

Li, V. C. and Yang, E., (2007). "Self healing in concrete materials." *In*: S. van der Zwaag Ed. *Self Healing Materials: An Alternative Approach to 20 Centuries of Materials Science*, Springer Series in Materials Science, 161-193.

Li, V. C. and Herbert, E. N., (2012). "Robust self-healing concrete for sustainable infrastructure." *Journal of Advanced Concrete Technology*, 10, 207-218.

Ozbay, E., Şahmaran, M., Lachemi, M. and Yucel, H. E., (2012). "Effect of microcracking on the frost durability of high volume fly ash and slag incorporated ECC." *ACI Materials Journal,* In Press.

Ozbay, E., Şahmaran, M., Lachemi, M. and Yucel, H. E., (2013). "Self-healing of microcracks in high volume fly ash incorporated engineered cementitious composites." *ACI Materials Journal*, 110(1), 1-11.

Qian, S., Zhou, J., De Rooij, M., Ye, G., Schlangen, E. and van Breugel, K., (2009). "Self-healing behavior of strain hardening cementitious composites incorporating local waste materials." *Cement and Concrete Composites*, 31(9), 613-621.

Reinhardt, H. W. and Jooss, M., (2003). "Permeability and self-healing of cracked concrete as a function of temperature and crack width." *Cement and Concrete Research*, 33(7), 981-985.

Şahmaran, M. and Li, V. C., (2009). "Durability properties of micro-cracked ECC containing high volumes fly ash." *Cement and Concrete Research*, 39(11), 1033-1043.

Şahmaran, M. and Li, V. C., (2010). "Engineered cementitious composites: Can composites be accepted as a crack-free concrete?" *Journal of Transportation Research Record*, 2164, 1-8.

Şahmaran, M., Yıldırım, G. and Erdem, T. K., (2013). "Self-healing capability of cementitious composites incorporating different supplementary cementitious materials." *Cement and Concrete Composites,* 35(1), 89-101.

Wang, S. and Li, V. C., (2007). "Engineered cementitious composites with high-volume fly ash." *ACI Materials Journal*, 104(3), 233-241.

Yamamoto, A., Watanabe, K., Li, V. C. and Niwa, J., (2010). "Effect of wet-dry condition on self-healing property of early-age ECC." *Proceedings of the Japan Concrete Institute*, 32(1), 251-256. (in Japanese)

Yang, E. H., Yang, Y. and Li, V. C., (2007). "Use of high volumes of fly ash to improve ECC mechanical

properties and material greenness." *ACI Materials Journal*, 104(6), 620-628.

Yang, Y., Lepech, M. D., Yang, E. H. and Li, V. C., (2009a). "Autogenous healing of engineered cementitious composites under wet-dry cycles." *Cement and Concrete Research*, 39(5), 382-390.

Yang, E., Şahmaran, M., Yang, Y. and Li, V. C., (2009b). "Rheological control in the production of engineered cementitious composites." *ACI Materials Journal*, 106(4), 357-366.

Zhong, W. and Yao, W., (2008). "Influence of damage degree on self-healing of concrete." *Construction and Building Materials*, 22(6), 1137-1142.

Zhou, J., Qian, S., Beltran, M. G. M., Ye, G., van Breugel, K. and Li, V. C., (2010). "Development of engineered cementitious composites with limestone powder and blast furnace slag." *Materials and Structures*, 43, 803-814.